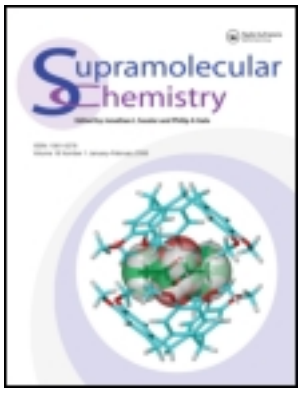

Supramolecular Chemistry
Publication details, including instructions for authors and subscription information:
http://www.tandfonline.com/loi/gsch20

Supramolecular hybrid nanomaterials as drug delivery systems

Mohsen Adeli [a b], Farahman Hakimpour [a], Massoumeh Sagvand [a], Mahmoud R. Jaafari [c], Roya Kabiri [d] & Zahra Moshari [a c]

[a] Department of Chemistry, Faculty of Science, Lorestan University, Khoramabad, Iran

[b] Department of Chemistry, Sharif University of Technology, Tehran, Iran

[c] School of Pharmacy, Nanotechnology and Biotechnology Research Center, Mashhad University of Medical Sciences, Mashhad, Iran

[d] Faculty of Chemistry, University of Tabriz, Tabriz, Iran

Available online: 15 Apr 2011

To cite this article: Mohsen Adeli, Farahman Hakimpour, Massoumeh Sagvand, Mahmoud R. Jaafari, Roya Kabiri & Zahra Moshari (2011): Supramolecular hybrid nanomaterials as drug delivery systems, Supramolecular Chemistry, 23:6, 411-418

To link to this article: http://dx.doi.org/10.1080/10610278.2010.531137

Supramolecular Chemistry
Vol. 23, No. 6, June 2011, 411–418

Taylor & Francis
Taylor & Francis Group

Supramolecular hybrid nanomaterials as drug delivery systems

Mohsen Adeli[ab]*, Farahman Hakimpour[a], Massoumeh Sagvand[a], Mahmoud R. Jaafari[c], Roya Kabiri[d] and Zahra Moshari[ac]

[a]*Department of Chemistry, Faculty of Science, Lorestan University, Khoramabad, Iran;* [b]*Department of Chemistry, Sharif University of Technology, Tehran, Iran;* [c]*School of Pharmacy, Nanotechnology and Biotechnology Research Center, Mashhad University of Medical Sciences, Mashhad, Iran;* [d]*Faculty of Chemistry, University of Tabriz, Tabriz, Iran*

(*Received 26 May 2010; final version received 28 September 2010*)

Highly fluorescent and water-soluble cadmium selenide quantum dots (QDs) functionalised by thio-cyclodextrin (HS-CD) and mercaptoacetic acid (MAA) as surface coating agents (QDs-CD-MAA) were synthesised successfully. The synthesised hybrid nanomaterials, QDs-CD-MAA, were able to form water-soluble complexes with paclitaxel and folic acid. QDs and their complexes were characterised by usual spectroscopy and microscopy methods. Size and morphology of functionalised QDs were dependent on their capping agents and guest molecules. Short-term *in vitro* cytotoxicity tests on mouse tissue connective fibroblast adhesive cells (L929) showed that conjugation of CD molecules onto the surface of QDs increases the rate of their internalisation into the cells, more than two times, compared with that without conjugated CD molecules. To prove the efficacy of functionalised QDs-CD-MAA and their host–guest systems, we subjected them to the endocytosis inside the cancer cells (tumour cell lines c26), then it was unambiguously proved that conjugation of CD molecules onto the surface of QDs increases the internalisation of anti-cancer drugs into the cells and consequently killing of cancer cells, thereby forming a solid foundation for further investigation and development.

Keywords: hybrid nanomaterials; quantum dots; anti-cancer; cyclodextrin; drug delivery; paclitaxel

Introduction

Quantum dots (QDs) are hybrid organic/inorganic nanomaterials with unique optical properties in which at least one physical dimension is smaller than the exciton Bohr radius (*1*, *2*). They provide a good opportunity to investigate the evolution of the properties of materials from bulk to nanoscale (*3*). When the size of a particle is reduced to less than the Bohr radius of the material a quantum confinement effect happens, which makes the bandgap energy dependent on particle size (*4*). The size and composition of nanoparticles can be varied to obtain emission wavelengths from blue to near-infrared (IR) (*5*); therefore, their fluorescence excitation and emission can be 'tuned' by altering the size of particles. The surface of the colloidal QDs used for medical applications is usually capped with organic ligands (*6*). One end of these organic ligands is connected to quantum dot surface and the other end is hydrophilic and may also be reactive to biomolecules (*7*). The effect of these conjugated ligands on the photoluminescence (PL) and other properties of QDs has been used to investigate the nature of their surface (*8*). In addition to their affect on the PL of QDs, introduction of the organic ligands onto the surface of nanoparticles improves the stability of these nanoentities in different solvents, increases solubility, prevents QD–QD interactions and the desired surface functionality, and sometimes reduces toxicity (*6–8*). Thiols are very useful materials that can be attached to QDs surface because they have high affinity for thiol ligands. Varieties of functional hydrophilic groups are attached to their surface to achieve water solubility and high functionality (*9*, *10*). However, in addition to organic capping agents, the structure of QDs should be modified by different modifier molecules or macromolecules such as biomolecules, antibodies, therapeutic agents and polymers, in order to improve their properties for biomedical applications (*11*). Many strategies have now been explained to obtain bioconjugated QD probes including both covalent and non-covalent interactions of proteins and other biomolecules at the QDs surface (*12*). One of the most important advantages of QDs in nanomedicine over current techniques is their ability to track cells *in vivo* easily and without the need to sacrifice the animals (*13*).

In order to use QDs in biomedical applications, several critical factors including water dispersibility, biocompatibility, chemical stability and robust optical properties should be taken into account (*14*). Among the many nanocrystals, cadmium selenide (CdSe) QDs are perhaps the most thoroughly studied nanocrystal system for biomedical applications (*15*). To achieve good water solubility and to improve the properties of CdSe QDs, these particles could be modified by biocompatible macromolecules such as cyclodextrins (CDs) (*16*). CDs are cyclic oligosaccharides which are naturally produced by the enzymatic conversion of starch and consisted of

*Corresponding author. Email: adeli@sharif.ir; mohadeli@yahoo.com

ISSN 1061-0278 print/ISSN 1029-0478 online

DOI: 10.1080/10610278.2010.531137
http://www.informaworld.com

glucose units, and these units are linked by 1,4-glycosidic bonds (*17*, *18*). Hydrophobic inside, hydrophilic outside and presence of two types of hydroxyl functional groups on the top and bottom of their nano-cavity make them unique candidates for a variety of applications ranging from drug delivery to molecular machines (*19*). CDs are used for a wide range of applications including pharmaceutical applications, fluorescence enhancement and solubility enhancement by inclusion complex formation (*18*).

Among the CDs family, β-CD and its derivatives are the best candidates for biomedical applications because the volume of their cavity matches the size of a large number of drugs (*20*).

CdSe QDs containing CD capping agents are suitable candidates in order to form complexes with biological ligands and anti-cancer drugs such as folic acid (FA) and paclitaxel (PTX).

FA is a water-soluble B vitamin and a ligand for cell surface receptors which can promote the formation of red blood cells. This ligand which is identified as an anti-anemia and growth factor is overexpressed in some of the human cancers including breast, ovarian, brain and kidney and is also expressed in some normal tissues (*21*, *22*).

PTX is an essential cytotoxic agent with a radius of <0.5 nm which is used in the treatment of different types of cancer (*23*, *24*). In the G2 phase of the cell mitotic cycle, PTX interacts with tubulin dimers to promote polymerisation of microtubules, which results in the formation of highly stable microtubules and thus prevents cell division (*25*). However, low aqueous solubility (about 0.3 μg/ml) is a major problem for PTX to be used in biological mediums (*23*, *26*). Many attempts have been made to improve the solubility of the PTX using various formulations, surfactants, PEGylated polymers, chremophor, solid dispersions, micro-nanoparticles and complexation with CDs (*26*). The ability of complex formation between modified β-CDs and PTX is investigated as a means to increase the water solubility of PTX (*27*).

In this work, a thiolated derivative of CD, SH-CD, was synthesised and used as capping agents to stabilise and functionalise CdSe QDs. Attachment of perthiolated β-CD onto the surface of CdSe QDs increases their sizes and changes their morphologies. The modified β-CD molecules which have been attached onto the QDs surface still retain their capability to form host–guest systems (*28*). The complexes of QDs with PTX and folic acid were prepared and characterised. Short-term *in vitro* cytotoxicity tests on mouse tissue connective fibroblast adhesive cells (L929) and investigation of the anti-cancer effect of functionalised QDs on tumour cell lines (c26) showed that conjugation of CD onto the surface of QDs increases the rate of internalisation of QDs into the cells several times more than that without conjugated CD molecules. On the basis of these results, QDs-CD-MAA and their host–guest systems are promising tumour-targeted imaging and drug delivery systems which can be used for early diagnosis and cancer therapy.

Methods

Triphenylphosphine was purchased from Merck and recrystallised in methanol prior to use. Thiourea and iodine were purchased from Sigma-Aldrich and used without further purification. DMF was purchased from Merck and distilled from CaH_2. β-CD was provided by Fluka and dried prior to use. $CdCl_2$ 2.5 H_2O, selenium powder, mercaptoacetic acid (MAA) and sodium sulphite were purchased from Sigma-Aldrich (St. Louis, MO, USA). Deionised water was used in all experiments.

A Shimadzu UV–vis 1650 PC spectrophotometer was used for recording absorption spectra in solution using a cell of 1.0 cm path length. A Varian Cary Eclipse fluorescence spectrophotometer was used for recording emission spectra in solution using a cell of 1.0 cm path length. IR spectra were recorded by a Nikolt 320 FT-IR using KBr tablets. Ultrasonic bath (Model: 5RS, 22 KHz, made in Italy) was used to disperse materials in solvents. Differential light scattering (DLS) thermograms were obtained using a Malvern-zs 20.4 in water solution. Samples of about 1 mg were placed in aluminium-type pans and were heated at the rate of 13–450°C/min. Differential scanning calorimetry (DSC) thermograms were recorded using TA-60 WS differential scanning calorimeter under air atmosphere. Samples of about 1 mg were placed in aluminium-type pans and were heated at the rate of 13–500°C/min. Ultrasonic bath (Model: 5RS, made in Italy) was used to disperse materials in solvents. ^{1}H NMR spectra were recorded in D_2O solvent on a Bruker DRX-400 (400 MHz) apparatus with the solvent proton signal as reference. The cell lines (mouse tissue connective fibroblast adhesive cells (L929) and tumour cell lines (c26)) were obtained from the National Cell Bank of Iran Pasteur Institute, Tehran, Iran. 3-(4,5-dimethylthiazol-2-yl)-2,5-diphenyltetrazolium bromide (MTT) powder, Annexin-V-FLUOS Staining Kit, was obtained from Sigma-Aldrich. Fluorescence images were recorded using a trinocular inverted microscope bright field and phase contrast motic Spain model: AE31.

Preparation of HS-CD

Synthesis of HS-CD is explained in detail in the Supporting Information, available online.

Preparation of CdSe QDs using MAA as capping agent (CdSe QDs-MAA)

CdSe QDs-MAA were prepared and purified according to the procedure in the literature (*30*).

Preparation of CdSe QDs using HS-CD as capping agent (CdSe QDs-CD)

Details are added to the Supporting Information, available online.

Preparation of QDs-CD-MAA

For preparation of CdSe QDs containing both MAA and CD capping agents, $CdCl_2.H_2O$ (0.684 g, 3.4 mmol) was dissolved in 50 ml distilled water at room temperature. Upon addition of MAA (0.3 ml, 4.31 mmol) to this solution, white colloids appeared. Then, HS-CD (0.025 g, 2 mmol) was added to this mixture and dispersed in the reaction mixture by stirring at room temperature. pH was brought to 11 by addition of NaOH (1 M) solution. Then, the mixture was placed in ultrasonic bath at 80°C for 15 min and water solution of Na_2SeSO_3 (0.1 M, 20 ml) was added to the reaction mixture. The mixture was left in ultrasonic bath for 30 min to obtain a yellow solution. The solution was stirred and heated at 90°C under N_2 atmosphere for 1 h, then it was cooled to room temperature and the product was separated through precipitation in acetone and then by centrifugation. Pure CdSe QDs-CD-MAA was obtained as a fine crystalline yellow compound after drying in a vacuum oven.

Preparation of QDs-CD-MAA and its inclusion complex with PTX (QDs-CD-MAA/PTX)

QDs-CD-MAA (0.05 g) was dissolved in 15 ml water. PTX powder (0.01 g, 10 mmol) was dissolved in 5 cc methanol and added to this solution. The mixture was left in an ultrasonic bath for 10 min, and then it was stirred in the dark at room temperature for at least 48 h. The solution was filtered and centrifuged, and the product was obtained as a yellow solid precipitate after drying in a vacuum oven.

Preparation of inclusion complex of QDs-CD-MAA/PTX with folic acid (QDs-CD-MAA/(PTX + FA))

QDs-CD-MAA/PTX (0.03 g) was dissolved in 10 ml water, and folic acid (0.005 g, 0.012 mmol) was added to this solution and the mixture was stirred in the dark at room temperature for 6 h. Then, the solution was filtered and the product was obtained as an orange powder upon centrifugation and drying in a vacuum oven.

Cell culture

Details are added to the Supporting Information, available online.

Cytotoxicity assay

In vitro cytotoxicity of the formulations and Taxol was determined by MTT assay (*31*). The cells (2500 cells/well) were seeded in 96-well plates. Various concentrations of carriers (0.03–10 μg/ml) or formulated PTX (1×10^{-4}–25.6 μg/ml) were then added to the wells in triplicates and incubated for 72 h. After the incubation period, 20 μl of MTT dye (5 mg/ml in PBS) was added to each well, and cells were incubated in the dark at 37°C for 5 h. Then the media were removed, and formazan crystals were dissolved in 200 μL dimethylsulphoxide and 20 μl of glycine buffer. Then, the absorbance of each well was measured by an ELISA reader (Stat Fax 2100 Awareness Technology, Palm city, FL, USA) at 570 nm.

Cell viability was calculated using the following equation:

$$\text{Cell viability}\,(\%) = (\text{Ints}/\text{Intscontrol}) \times 100,$$

where Ints is the colorimetric intensity of the cells incubated with the samples, and Intscontrol is the colorimetric intensity of the cells incubated with the media only (positive control).

Toxicity of the formulations was expressed as IC50 (inhibitory concentration required to cause a 50% of cell growth inhibition) which was calculated by the CalcuSyn software version 2.1 (Biosoft, Cambridge, UK). It is notable that owing to the absorption of vitamins, amino acids and ions at the surfaces of nanoparticles, it is clear that the common *in vitro* examination method can yield erroneous cell viability values (*32*, *33*).

In this study, in order to obtain a more reliable way of identifying cytotoxicity for *in vitro* assessments, we used surfaces of saturated nanoparticles via interactions with RPMI before usage according to the instruction in references.

Outlier detection

All MTT experiments were performed in triplicate or more, with the results expressed as mean ± standard deviation; standard deviation values are indicated as error bars in the MTT result plots. The results were statistically processed for outlier detection using a 'T procedure' (REF) using MINITAB software (Minitab Inc., State College, PA, USA). One-way analysis of variance (ANOVA) with $p < 0.05$ was performed for each set of MTT assay test repeats. Outlier samples were then excluded from the corresponding asset viability calculations (*34*).

In this method, a *T*-ratio is calculated as follows:

$$T = \frac{X - \bar{X}}{S},$$

where X is the suspected outlier point (normally the smallest or the largest value in a set of measurements), $\bar{X}$ is the sample mean and S is the (estimated) standard deviation. If the calculated value of T is equal to or exceeds

a critical value, the outlier point is removed with a significance level of 0.05. In the latter case, assuming that the data were sampled from a normal distribution, there is at least a 95% chance that the suspected point is in fact far from other points.

Results

CD was thiolated according to the procedure in the literature (*29*). According to this procedure, the I-CD was synthesised and then was reacted with thiourea to produce HS-CD (Supporting Information, available online, Scheme 1).

HS-CD is not a suitable capping agent for preparation of CdSe QDs solely because it has seven – SH functional groups that were attached to the several QDs and lead to a network probably.

A well-known capping agent for preparation of a variety of QDs is MAA which causes a good solubility in water. As explained above, synthesis of CdSe QDs using HS-CD capping agent failed. Hence, CdSe QDs containing MAA were synthesised and then reacted with HS-CD to introduce CD onto their surface through ligand exchange, but this reaction did not proceed. It seems that the bonding between cadmium atoms and SH groups (S atom) of MAA was ionic (or covalence) which was strong enough to avoid cleavage and was replaced by SH groups of HS-CD.

In contrast to the above procedures which failed to produce fine QDs containing CDs capping agents, another strategy in which a mixture of MAA and HS-CD was used as capping agent was carried out successfully. This method led to fine QDs containing CDs and MAA on their surface (QDs-CD-MAA). QDs-CD-MAA was able to form complexes with anti-cancer drugs and biological ligands such as PTX and folic acid (Supporting Information, available online, Figure 2).

As a result, capping of the surface of QDs by CD molecules leads to new imaging and drug delivery systems. QDs containing CDs as capping agent were completely water soluble, and they had a high loading capacity to transport anti-cancer drugs and biological ligands. Conjugation of CD molecules onto the surface of QDs increases the rate of crossing of the cell membrane by these nanomaterials.

MTT reduction was used to metabolically quantify viable cells after exposure to nanoparticles. As published reports confirm that the use of the MTT assay for measuring the toxicity of nanoparticles has high variability and non-specificity, the outlier detection method was applied to minimise variability (*35*). Several *in vitro* and *in vivo* studies by different groups have shown that CdSe QDs are toxic due to the release of cadmium ions. In order to evaluate the effect of conjugated CD molecules on the biocompatibility of QDs, we carried out MTT assay for QDs containing MAA capping agent, without conjugated CD molecules, and QDs having two different amounts of conjugated CD molecules. It was found that conjugation of the CD molecules onto the surface of QDs-MAA decreases the viability of the L929 cell line. A decrease in the viability of the cells upon conjugation of the CD molecules onto the surface of QDs can be assigned to the increase in the transfer of QDs through cell membrane. However, conjugation of a high number of CD molecules onto the surface of QDs increased their biocompatibility interestingly. In this case, inherent biocompatibility of CDs dominates the increase in the toxicity of QDs caused by the increase in their transfer to the cytoplasm (Supporting Information, available online, Figure 3). There is not a significance difference between cytotoxicity results after 3 and 24 h incubation. Therefore, it can be found that a majority of QDs pass through the cell membrane in less than 3 h.

Ability of QDs-CD-MAA and their host–guest systems as drug delivery systems to kill the cancer cells was studied. On the basis of *in vitro* studies on tumour cell line c26, it was found that QDs-CD-MAA/PTX were able to kill cancer cells effectively. Table 1 shows the inhibitory concentration of PTX, QDs-MAA, QDs-CD-MAA, QDs-CD-MAA/PTX and QDs-CD-MAA/(PTX + FA), producing 50% cell growth inhibition or death, IC50. The IC50 for QDs-CD-MAA/PTX is much lower than that for QDs-MAA and QDs-CD-MAA. It is also small for QDs-CD-MAA when compared with that for QDs-MAA. These results agree with the MTT results for the L929 cell line, because CD molecules always increase the ability of the QDs and their host–guest systems to cross the cell membrane. Figure 1 shows that 1 μg/ml of QDs-CD-MAA/PTX kills more that 80% of cancer cells. Although the cytotoxicity of the QDs-CD-MAA/(PTX + FA) versus cancer cells is much more than that of QDs-MAA and QDs-CD-MAA, it is still lower than QDs-CD-MAA/PTX. Complexation of FA molecules onto the surface of QDs-CD-MAA/PTX leads to the dissociation of some of the PTX molecules and decreases the number of the PTX molecules loaded onto the surface of QDs and consequently decreases the anti-cancer effect of the system. Due to the presence of conjugated CD molecules, the biocompatibility of QDs-CD-MAA in low concentrations (0.03 and 0.05 μg/ml) is always higher than that of QDs-MAA, outstandingly.

Discussion

The structure of QDs and guest molecules was evaluated using IR (Supporting Information, available online) and NMR spectroscopies. Figure 2 shows the ^{1}H NMR spectra of capping agent, functionalised QDs and their host–guest systems. In the ^{1}H NMR spectra of QDs-MAA, the signals at 3.19–3.71 ppm and 1.9 ppm are correspondent to the protons of CH_2 groups of the MAA which indicated that

Table 1. *In vitro* cytotoxicity of QDs-MAA, QDs-CD-MAA, QDs-CD-MAA/PTX, QDs-CD-MAA/(PTX + FA) and PTX on the tumour cell line (c26).

Sample	Tumour cell lines c26 (IC50 μg/ml)
QDs-MAA	0.63
QDs-CD-MAA	3.02
QDs-CD-MAA/PTX	0.05
QDs-CD-MAA/(PTX + FA)	0.36
PTX	0.029

MAA is connected to the surface of QDs. After attachment of the CD to the surface of QDs, signals of MAA capping agent appeared at 3.22–3.37 ppm, but they are broader than that of QDs-MAA. Formation of the inclusion complexes between PTX and CD molecules conjugated onto the surface of QDs was also indicated by NMR spectroscopy. There are distinct differences in the proton spectra of QDs-CD-MAA and QDs-CD-MAA/PTX, which confirm the presence of PTX onto the surface of QDs. The presence of the signals of PTX protons in this spectrum proves complexation of PTX by QDs-CD-MAA. ^{1}H NMR spectra of the QDs-CD-MAA/(PTX + FA) are also displayed in Figure 2. In this spectrum, aromatic and hydroxyl protons of FA appears at 7–8 and 8–10 ppm, respectively.

Conjugation of CD molecules onto the surface of QDs was proved through comparison of the thermal behaviours of pristine materials, intermediates and final products. DSC thermograms of β-CD, I-CD and HS-CD are shown in the Supporting Information, available online in Figure 5. The DSC curve of β-CD shows an endothermic peak at about 100°C due to release of water molecules and an exothermic peak at 350–400°C assigned to the decomposition of this compound. Prior to this transition, an endothermic peak observed at 310°C corresponds to

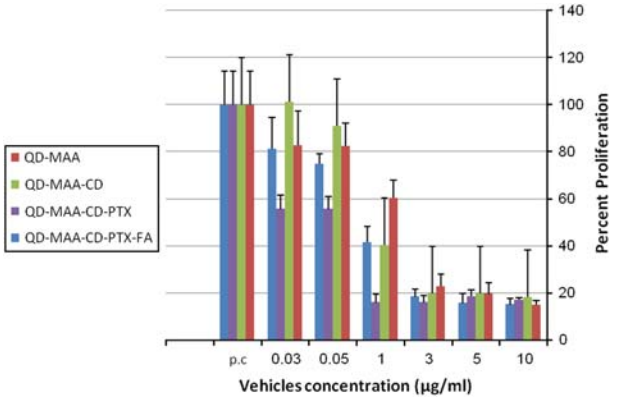

Figure 1. Effect of the concentration of QDs-MAA, QDs-CD-MAA, QDs-CD-MAA/PTX and QDs-CD-MAA/(PTX + FA) on the viability of tumour cell line (c26) after 3 and 24 h incubation (MTT assay).

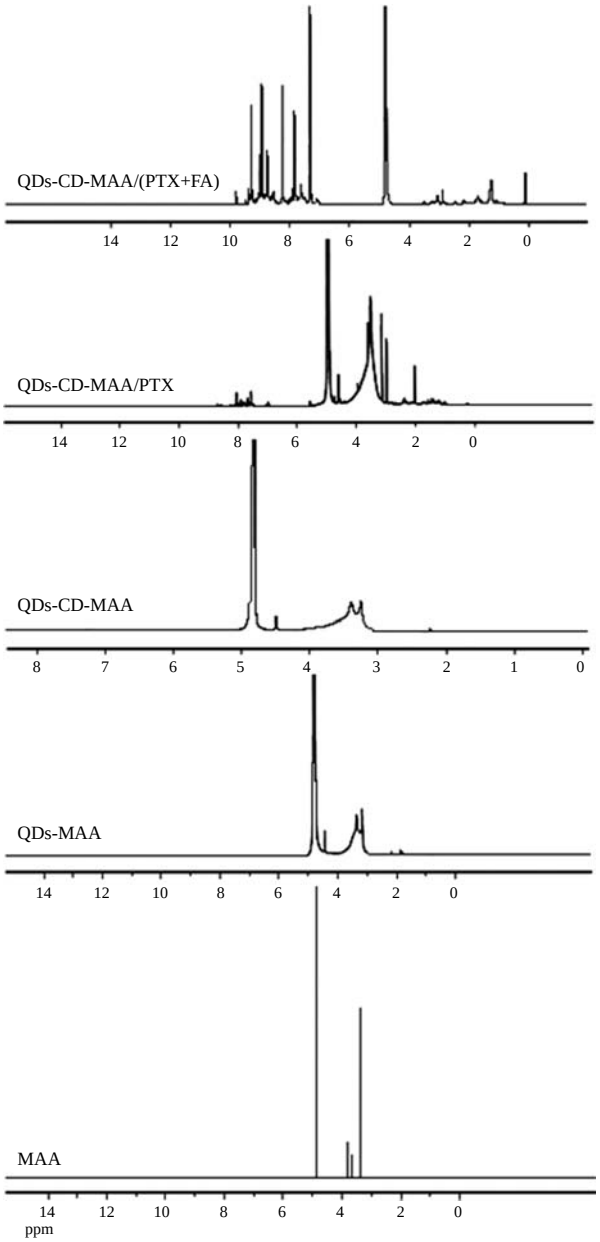

Figure 2. ^{1}H NMR spectra of QDs-MAA, QDs-CD-MAA, QDs-CD-MAA/PTX and QDs-CD-MAA/(PTX + FA).

the crystallisation point of the compound. However, disappearance of the exothermic peak at 350–400°C (corresponds to the decomposition temperature of β-CD) and appearance of a new exothermic peak at 230°C (assigned to the decomposition temperature of I-CD) in the DSC thermogram of I-CD indicate the formation of this compound. Thiolation of I-CD and preparation of HS-CD were followed by the comparison of their DSC thermograms, where the characteristic peak of I-CD (appeared at 230°C) disappeared and a new exothermic peak at 300°C for decomposition of HS-CD appeared. Considerable difference between the decomposition temperature of

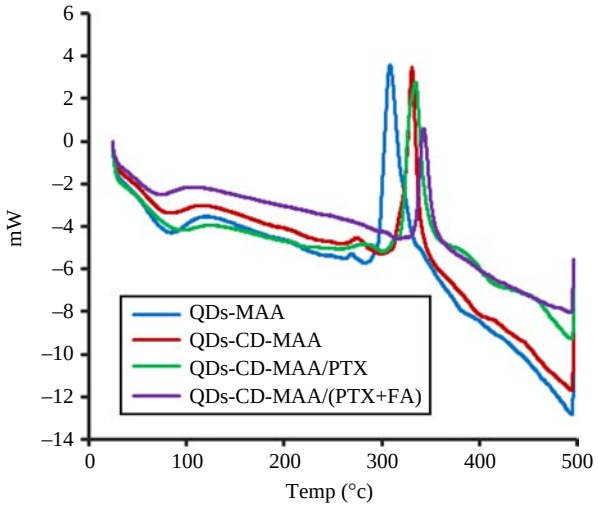

Figure 3. DSC thermograms of QDs-MAA, QDs-CD-MAA, QDs-CD-MAA/PTX and QDs-CD-MAA/(PTX + FA).

capping agents of QDs-MAA and QDs-CD-MAA confirmed conjugation of CD molecules onto the surface of QDs. The peaks assigned to these temperatures can be seen at 310 and 340°C for QDs-MAA and QDs-CD-MAA, respectively (Supporting Information, available online, Figure 6).

This method was also used to prove the formation of inclusion complex between QDs-CD-MAA and PTX molecules, where the decomposition temperature of QDs-CD-MAA was raised to about 7°C upon complexation with PTX molecules. To ensure the formation of inclusion complex between QDs-CD-MAA and PTX molecules, we recorded the DSC thermogram of physical mixture of QDs-CD-MAA and PTX and compared them with those of inclusion complex and PTX. As it can be seen in Figure 7 of Supporting Information, available online, the DSC thermogram of physical mixture shows both decomposition temperatures of PTX and QDs-CD-MAA, whereas this is not observed in the DSC thermogram of inclusion complex. By comparing the DSC thermograms of QDs-CD-MAA/PTX, QDs-CD-MAA/(PTX + FA), physical mixture of QDs-CD-MAA/PTX and FA and also FA, it can be found that they have different decomposition

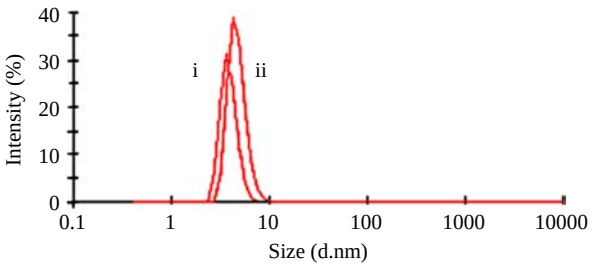

Figure 4. DLS diagrams of (i) QDs-MAA and (ii) QDs-CD-MAA.

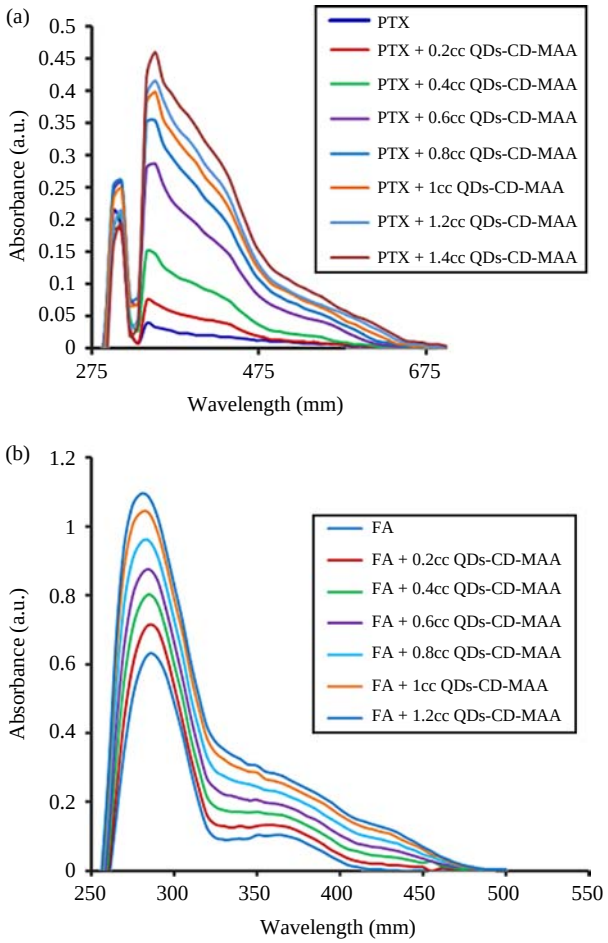

Figure 5. UV–vis spectra of PTX upon addition of different concentrations of (a) QDs-MAA and QDs-CD-MAA solutions (b) UV–vis spectra of FA upon addition of different concentrations of (c) QDs-MAA and (d) QDs-CD-MAA solutions.

temperatures. This result proves that folic acid is also complexed to the QDs-CD-MAA/PTX (Supporting Information, available online, Figure 8).

Differences between the decomposition temperatures of capping agents of synthesised hybrid nanomaterials and their complexes, without pristine materials, intermediates and physical mixtures, for a better understanding, are displayed in Figure 3.

Size of QDs-MAA, QDs-CD-MAA, QDs-CD-MAA/PTX and QDs-CD-MAA/(PTX + FA) was determined using DLS experiments.

DLS experiments show an increase in the size of CdSe QDs upon conjugation of CDs onto their surface. According to these experiments, sizes of QDs-MAA and QDs-CD-MAA were 5.5 and 7.5 nm, respectively (Figure 4).

Figure 10 in Supporting Information, available online, shows the UV–vis spectra of QDs-MAA, QDs-CD-MAA,

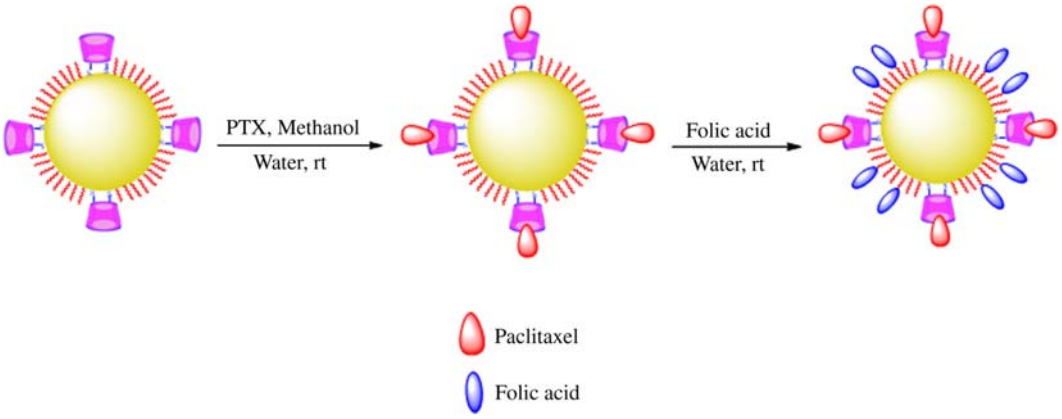

Figure 6. Complexation of FA and PTX to the surface of QDs-CD-MAA through different interactions.

QDs-CD-MAA/PTX and QDs-CD-MAA/(PTX + FA). Conjugation of CD molecules onto the surface of QDs-MAA have caused a red shift for plasmon absorbance peaks from 363 and 400 nm for QDs-MAA to 392 and 425 nm for QDs-CD-MAA, meaning that attachment of CD molecules onto the surface of QDs-MAA results in the increase in the size of the QDs. Complexation of PTX and FA to QDs-CD-MAA causes a red shift in its plasmon absorbance peaks to 395 and 433 nm for QDs-CD-MAA/PTX and to 365 and 424 nm for QDs-CD-MAA/(PTX + FA).

Figure 11(a),(b) in Supporting Information, available online, shows the photograph of water solutions of QDs-MAA and QDs-CD-MAA under sunlight, respectively, and Figure 11(c),(d) shows the same samples under UV radiation.

Figure 12 in Supporting Information, available online, shows the PL spectra of QDs-MAA, QDs-CD-MAA, QDs-CD-MAA/PTX and QDs-CD-MAA/(PTX + FA) excited at 450 nm. All samples have a broad emission between 465 and 850 nm with a red shift upon conjugation of CD or complexation of guests to QDs.

The formation of inclusion complexes between guests, PTX and FA, and hosts, QDs-MAA and QDs-CD-MAA, was evaluated by UV–vis experiments. The intensity of the λ_{max} of UV absorption of guests increased upon addition of the hosts, confirming creation of inclusion complexes between FA and PTX with conjugated CD molecules onto the surface of QDs (Figure 5(a),(b)). Raising of the maximum absorption of the guest molecules upon addition of QDs-MAA, without conjugated CDs, showed that QDs transport guest molecules not only through inclusion complexes but also through other interactions such as hydrogen bonding and electrostatic interactions (Supporting Information, available online, Figure 13(a),(b)) (Figure 6).

To prove the host–guest relationship between FA and QDs-MAA and QDs-CD-MAA, we recorded UV–vis spectra of QDs-MAA and QDs-CD-MAA in the presence of different concentrations of FA. Due to the interaction of FA with QDs-MAA and QDs-CD-MAA and better dispersion in solution, their maximum absorption increases in both cases (Supporting Information, available online, Figure 14).

References

(1) Dorokhin, D.; Tomczak, N.; Han, M.; Reinhoudt, D.N.; Velders, A.H.; Vancso, G.J. *ACS nano.* **2009**, *3*, 661–667.
(2) Jones, M.; Kumar, S.; Lo, S.S.; Scholes, G.D. *J. Phys. Chem. C* **2008**, *112*, 5423–5431.
(3) Yu, K.; Ouyang, J.; Zaman, M.B.; Johnston, D.; Yan, F.J.; Li, G.; Ratcliffe, C.I.; Leek, D.M.; Wu, X.; Stupak, J.; Jakubek, Z.; Whitfield, D. *J. Phys. Chem. C* **2009**, *113*, 3390–3401.
(4) Rzigalinski, B.A.; Strobl, J.S. *Toxicol. Appl. Pharmacol.* **2009**, *238*, 280–288.
(5) Bentzen, E.L.; Tomlinson, I.D.; Mason, J.; Gresch, P.; Warnement, M.R.; Wright, D.; Sanders-Bush, E.; Blakely, R.; Rosenthal, S.J. *Bioconjug. Chem.* **2005**, *16*, 1488–1494.
(6) Kilina, S.; Ivanov, S.; Tretiak, S. *J. Am. Chem. Soc.* **2009**, *131*, 7717–7726.
(7) Yu, W.W.; Chang, E.; Drezek, R.; Colvin, V.L. *Biochem. Biophys. Res. Commun.* **2006**, *348*, 781–786.
(8) Zhang, Y.; Jing, P.; Zeng, Q.; Sun, Y.; Su, H.; Wang, Y.A.; Kong, X.; Zhao, J.; Zhang, H. *J. Phys. Chem. C* **2009**, *113*, 1886–1890.
(9) Zhou, D.; Ying, L.; Hong, X.; Hall, E.A.; Abell, C.; Klenerman, D. *Langmuir* **2008**, *24*, 1659–1664.
(10) Jamieson, T.; Bakhshi, R.; Petrova, D.; Pocock, R.; Imani, M.; Seifalian, A.M. *Biomaterials* **2007**, *28*, 4717–4732.
(11) (a) Sunderland, C.J.; Steiert, M.; Talmadge, J.E.; Derfus, A.M.; Barry, S.E. *Drug Dev. Res.* **2006**, *67*, 70–93. (b) Smith, A.M.; Ruan, G.; Rhyner, M.N.; Nie, S. *Ann. Biomed. Eng.* **2006**, *34*, 3–14.
(12) Dif, A.; Boulmedais, F.; Pinot, M.; Roullier, V.; Baudy-Floc'h, M.; Coquelle, F.M.; Clarke, S.; Neveu, P.; Vignaux, F.; Borgne, R.L.; Dahan, M.; Gueroui, Z.; Marchi-Artzner, V. *J. Am. Chem. Soc.* **2009**, *131*, 14738–14739.
(13) (a) Shi, C.; Zhu, Y.; Xie, Z.; Qian, W.; Hsieh, C.-L.; Nie, S.; Su, Y.; Zhau, H.E.; Chung, L.W.K. *Urology* **2009**, *74*, 446. (b) Gao, X.; Cui, Y.; Levenson, R.M.; Chung, L.W.K.; Nie, S. *Nat. Biotechnol.* **2004**, *22*, 969–976.

(14) Daou, T.J.; Li, L.; Reiss, P.; Josserand, V.; Texier, I. *Langmuir* **2009**, *25*, 3040–3044.
(15) Deka, S.; Quarta, A.; Lupo, M.G.; Falqui, A.; Boninelli, S.; Giannini, C.; Morello, G.; Giorgi, M.D.; Lanzani, G.; Spinella, C.; Cingolani, R.; Pellegrino, T.; Manna, L. *J. Am. Chem. Soc.* **2009**, *131*, 2948–2958.
(16) Li, H.; Han, C. *Chem. Mater.* **2008**, *20*, 6053–6059.
(17) Yildiz, H.B.; Tel-Vered, R.; Willner, I. *Angew. Chem. Int. Ed.* **2008**, *47*, 6629–6633.
(18) Liu, J.-H.; Chiu, Y.-H.; Chiu, T.-H. *Macromolecules* **2009**, *42*, 3715–3720.
(19) Adeli, M.; Zarnegar, Z.; Kabiri, R. *Eur. Polym. J.* **2008**, *44*, 1921–1930.
(20) Cai, W.; Sun, T.; Liu, P.; Chipot, C.; Shao, X. *J. Phys. Chem. B* **2009**, *113*, 7836–7843.
(21) Wang, Y.; Zheng, J.; Zhang, Z.; Yuan, C.; Fu, D. *Colloids and Surfaces A: Physicochem. Eng. Asp.* **2009**, *342*, 102–106.
(22) Sewell, S.L.; Giorgio, T.D. *Mater. Sci. Eng.* **2009**, *29*, 1428–1432.
(23) Boquet, W.; Boterberg, T.; Ceelen, W.; Pattyn, P.; Peeters, M.; Bracke, M.; Remon, J.P.; Vervaet, C. *Int. J. Pharm.* **2009**, *367*, 148–154.
(24) Peng, L.; Mendelsohn, A.D.; Latempa, T.J.; Yorlya, S.; Grimes, C.A.; Desal, T.A. *Nano. Lett.* **2009**, *9*, 1932–1936.
(25) Obara, K.; Ishihara, M.; Ozeki, Y.; Ishizuka, T.; Hayashi, T.; Nakamura, S.; Saito, Y.; Yura, H.; Matsui, T.; Hattori, H.; Takase, B.; Ishihara, M.; Kikuchi, M.; Maehara, T. *J. Control. Release* **2005**, *110*, 79–89.
(26) Khandare, J.J.; Jayant, S.; Singh, A.; Chanda, P.; Wang, Y.; Vorsa, N.; Minko, T. *Bioconjug. Chem.* **2006**, *17*, 1464–1472.
(27) Bouquet, W.; Ceelen, W.; Fritzinger, B.; Pattyn, P.; Peeters, M.; Remon, J.P.; Vervaet, C. *Eur. J. Pharm. Biopharm.* **2007**, *66*, 391–397.
(28) Palaniappan, K.; Xue, C.; Arumugam, G.; Hackney, S.A.; Liu, J. *Chem. Mater.* **2006**, *18*, 1275–1280.
(29) Benkhaled, A.; Cheradame, H.; Fichet, O.; Teyssié, D.; Buchmann, W.; Guégan, P. *Carbohydr. Polym.* **2008**, *73*, 482–489.
(30) Han, H.-Y.; Sheng, Z.-H.; Liang, J.-G. *Mater. Lett.* **2006**, *60*, 3782–3785.
(31) Malaekeh-Nikouei, B.; Jaafari, M.R.; Sajadi Tabassi, S.A.; Samiei, A. *Colloids Surf. B: Biointerfaces* **2008**, *67*, 238–244.
(32) Mahmoudi, M.; Simchi, A.; Imani, M.; Shokrgozar, M.A.; Milani, A.S.; Häfeli, U.O.; Stroeve, P. *Colloids Surf. B: Biointerfaces* **2010**, *75*, 300–309.
(33) Mahmoudi, M.; Simchi, A.; Imani, M.; Milani, A.S.; Stroeve, P. *Nanotechnology* **2009**, *20*, 225104.
(34) Bolton, S.; Dekker, M. *Pharmaceutical Statistics: Practical and Clinical Applications*, 2nd ed.; Marcel Dekker: New York, 1990.
(35) Häfeli, U.; Pauer, G.J. *J. Magn. Magn. Mat.* **1999**, *194*, 76–82.